






Lysine demethylase LSD1 delivered via small extracellular vesicles promotes gastric cancer cell stemness

Li-Juan Zhao¹, Ying-Ying Li¹, Yu-Tong Zhang¹, Qi-Qi Fan¹, Hong-Mei Ren¹, Cheng Zhang² , Adil Mardinoglu^{2,3} , Wen-Chao Chen⁴ , Jing-Ru Pang¹, Dan-Dan Shen¹, Jun-Wei Wang¹, Long-Fei Zhao¹, Jian-Ying Zhang⁵, Zhen-Ya Wang⁶, Yi-Chao Zheng^{1,*}  & Hong-Min Liu^{1,**} 

Abstract

Several studies have examined the functions of nucleic acids in small extracellular vesicles (sEVs). However, much less is known about the protein cargos of sEVs and their functions in recipient cells. This study demonstrates the presence of lysine-specific demethylase 1 (LSD1), which is the first identified histone demethylase, in the culture medium of gastric cancer cells. We show that sEVs derived from gastric cancer cells and the plasma of patients with gastric cancer harbor LSD1. The shuttling of LSD1-containing sEVs from donor cells to recipient gastric cancer cells promotes cancer cell stemness by positively regulating the expression of Nanog, OCT4, SOX2, and CD44. Additionally, sEV-delivered LSD1 suppresses oxaliplatin response of recipient cells *in vitro* and *in vivo*, whereas LSD1-depleted sEVs do not. Taken together, we demonstrate that LSD1-loaded sEVs can promote stemness and chemoresistance to oxaliplatin. These findings suggest that the LSD1 content of sEV could serve as a biomarker to predict oxaliplatin response in gastric cancer patients.

Keywords gastric cancer; LSD1; small extracellular vesicles; stemness

Subject Categories Cancer; Membranes & Trafficking; Post-translational Modifications & Proteolysis

DOI 10.15252/embr.202050922 | Received 20 May 2020 | Revised 8 May 2021 |

Accepted 11 May 2021 | Published online 31 May 2021

EMBO Reports (2021) 22: e50922

Introduction

Gastric cancer, which is the fifth most frequently diagnosed cancer and the third leading cause of cancer-related deaths worldwide,

accounted for more than one million new cases and 783,000 estimated deaths in 2018 (Bray *et al*, 2018). The incidence of gastric cancer and gastric cancer-related mortality are declining globally. However, the incidence of gastric cancer is high in several parts of the world, especially in East Asia and South America (Van Cutsem *et al*, 2016). The therapeutic strategies for gastric cancer include surgery and chemotherapy (Takahashi *et al*, 2013). However, the current chemotherapy regimens for gastric cancer have limited efficacy as they do not mitigate tumor recurrence, which is partially due to the persistence of cancer stem cells (CSCs) (Enjoji *et al*, 2018; Huang *et al*, 2019). The molecular mechanisms underlying cancer stemness have not been completely elucidated.

In multicellular organisms, distant cells can interact through various molecules or extracellular vesicles (EVs) harboring unique proteins, lipids, and nucleic acids (Tkach & Thery, 2016). The secreted EVs are detected in the urine, amniotic fluid, bronchoalveolar lavage fluid, breast milk, saliva, and blood. Small EVs (sEVs) are the smallest subset of EVs with a size ranging from 50 to 150 nm (EL Andaloussi *et al*, 2013). Various proteins and nucleic acids are packed into the sEVs. The fusion of sEVs to the target cells enables the delivery of molecular cargos to the recipient cells. Hence, sEVs are important mediators of cell-to-cell communication.

Recent studies have suggested that the sEV-related nucleic acids, such as microRNAs (miRNAs) and messenger RNAs (mRNAs), which mediate various signaling processes, are potential diagnostic and prognostic biomarkers for cancer (Valadi *et al*, 2007; Wang *et al*, 2010; Ono *et al*, 2014; Singh *et al*, 2014; Bao *et al*, 2018). However, limited studies have examined the proteins within sEVs. sEVs harbor several proteins, such as β -catenin (Chairoungdua *et al*, 2010), EGFR (Zhang *et al*, 2017a), PD-L1 (Chen *et al*, 2018), p65 and p53 (Yang *et al*, 2017), DNMT1 (Cao *et al*, 2017),

1 State Key Laboratory of Esophageal Cancer Prevention & Treatment, Key Laboratory of Advanced Drug Preparation Technologies, Ministry of Education of China, Collaborative Innovation Center of New Drug Research and Safety Evaluation, Henan Province, Key Laboratory of Henan Province for Drug Quality and Evaluation, Institute of Drug Discovery and Development, School of Pharmaceutical Sciences, Academy of Medical Science, Zhengzhou University, Zhengzhou, China

2 Science for Life Laboratory, KTH – Royal Institute of Technology, Stockholm, Sweden

3 Faculty of Dentistry, Oral & Craniofacial Sciences, Centre for Host-Microbiome Interactions, King's College London, London, UK

4 Department of Gastrointestinal Surgery, Henan Provincial People's Hospital, People's Hospital of Zhengzhou University, Zhengzhou, China

5 Henan Institute of Medical and Pharmaceutical Sciences, Zhengzhou University, Zhengzhou, China

6 Key Laboratory of "Runliang" Antiviral Medicines Research and Development, Institute of Drug Discovery & Development, Zhengzhou University, Zhengzhou, China

*Corresponding author. Tel.: +86 15036157387; E-mail: yichaozheng@zzu.edu.cn

**Corresponding author. Tel.: +86 13603980340; E-mail: liuhm@zzu.edu.cn

Notch3 (Lin *et al*, 2019), Claudin (Li *et al*, 2009), and Wnt10b (Chen *et al*, 2017). Additionally, previous studies have reported that sEVs comprise several transcriptional regulators and that mRNAs and proteins within sEVs are involved in both the response to environmental stimuli and epigenetic modifications, especially histone modification (Ung *et al*, 2014; Qian *et al*, 2015). Studies on the functions of histone demethylases, which are one of the sEV cargos, are limited.

This study demonstrated that the histone demethylase LSD1, which functions as an oncogene in gastric cancer (Huang *et al*, 2007; Wang *et al*, 2009; Kontaki & Talianidis, 2010; Zheng *et al*, 2016b; Li *et al*, 2017), is enriched in sEVs from gastric cancer cells and plasma of patients with gastric cancer. The sEV cargos, including LSD1, can be transferred from the parent to recipient gastric cancer cells and enhance their stemness and suppress chemosensitivity *in vitro* and *in vivo*. Conversely, sEVs lacking LSD1 do not promote gastric cell stemness or suppressed chemosensitivity. The findings of this study demonstrated that LSD1 is delivered through sEVs. Additionally, this study elucidated a critical non-canonical pathway of LSD1 that promotes gastric cancer carcinogenesis by functioning as a secreted protein instead of a nuclear protein.

Results

LSD1 is secreted through sEVs from gastric cancer cells

Cells secrete various growth factors or EVs during growth. Hence, the morphology of cells may change upon stimulation with cargos secreted into the cell culture medium. In this study, conditioned medium from the gastric cancer cell line MGC-803 promoted sphere formation, which is a characteristic feature of cancer cell stemness, in the recipient gastric cancer cells (Fig 1A). Hence, we hypothesized that some specific components in conditioned medium may contribute to cancer cell stemness. sEVs are one of the potential components in the conditioned medium that contribute to cancer cell stemness as they have critical roles in intercellular

communication (Chaput & Thery, 2011; Lee *et al*, 2012). To verify this hypothesis, a sphere formation assay was performed using GW4869 (10 μ M), an inhibitor of sEV biogenesis and secretion (Jiang *et al*, 2017; Faict *et al*, 2018). Treatment with GW4869 mitigated the conditioned medium-induced enhanced sphere formation to a level observed in the cells incubated in fresh medium (Fig 1B). Therefore, these data indicate that sEVs may contribute to gastric cancer cell stemness. To further confirm the role of sEVs in gastric cancer cell stemness, the MGC-803 cells were treated with sEVs isolated using differential ultracentrifugation (sEV fraction) or the supernatant of differential ultracentrifugation (sEV-lacking fraction). sEV-treated cells exhibited enhanced sphere-forming ability (Fig 1C). The sEV marker proteins were detected using Western blotting to examine the number of sEVs secreted from equal numbers of cells. GW4869 effectively inhibited the secretion of sEVs from the gastric cancer cells (Fig EV1A). The number of sEVs secreted from the GW4869-treated cells was lower than that secreted from the untreated cells. Additionally, treatment with GW4869 decreased the number of sEVs released from the same number of cells and consequently inhibited sphere formation in the recipient cells (Fig EV1B). Furthermore, sEVs dose-dependently promoted sphere formation in recipient cells (Fig EV1C). Thus, gastric cancer cell-derived sEVs promoted gastric cancer cell stemness.

The ability of sEVs from diverse gastric cancer cells to promote sphere formation is unclear owing to their complexity and heterogeneity. Therefore, the MGC-803 cells were treated with an equal number of sEVs (determined based on the protein levels) derived from five representative gastric cell lines. As shown in Fig 1D, only sEVs derived from MGC-803, HGC-27, and BGC-823 cells promoted sphere formation in the recipient cells. The data shown in Fig 1E (left panel) indicate that these cell lines exhibit LSD1 overexpression, which is consistent with the results of previous studies (Zheng *et al*, 2013). LSD1, which is reported to promote cancer cell stemness (Amente *et al*, 2013; Lei *et al*, 2015), has been considered as a drug target (Zheng *et al*, 2016a; Sun *et al*, 2017; Zheng *et al*, 2017; Duan *et al*, 2018; Liu *et al*, 2019). Previous studies have predicted that LSD1 is a secretory protein using Phobius (Kall *et al*, 2007) and

Figure 1. LSD1 is secreted from gastric cancer cells through small extracellular vesicles (sEVs).

- A Sphere formation in MGC-803 cells incubated with fresh medium or conditioned medium from MGC-803 cells for 7 days. The number of spheres was quantified and indicated on the right. Scale bar = 100 μ m ($n = 3$ biological replicates; mean \pm standard error of mean (SEM); * $P = 0.0146$; two-tailed unpaired Student's t -test).
- B Sphere formation in MGC-803 cells with indicated treatment. The number of spheres was quantified and indicated on the right. Scale bar = 100 μ m ($n = 3$ biological replicates; mean \pm SEM; no significant differences; two-tailed unpaired Student's t -test).
- C Sphere formation in MGC-803 cells incubated with an equal volume of phosphate-buffered saline, supernatant after differential centrifugation, or sEVs. Scale bar = 100 μ m ($n = 3$ biological replicates; mean \pm SEM; ns, no significant difference; * $P = 0.0390$; two-tailed unpaired Student's t -test).
- D Sphere formation in MGC-803 cells treated with sEVs (20 μ g/ml) from five gastric cancer cell lines as indicated ($n = 3$ biological replicates; mean \pm SEM; *** $P = 0.0007$ (MGC-803), ** $P = 0.0061$ (HGC-27), and ** $P = 0.0018$ (BGC-823); two-tailed unpaired Student's t -test).
- E Expression levels of LSD1 in MGC-803, MKN-45, HGC-27, BGC-823, and NCI-N87 cell lines and their corresponding sEVs. The samples with equal amounts of proteins were loaded ($n = 3$ biological replicates; mean \pm SEM; compared with the NCI-N87; * $P = 0.0432$ (cell/MGC-803), * $P = 0.0300$ (cell/HGC-27), ** $P = 0.0306$ (cell/BGC-823), ** $P = 0.0018$ (sEVs/MGC-803), ** $P = 0.0029$ (sEVs/HGC-27), and *** $P = 0.0003$ (sEVs/BGC-823); two-tailed unpaired Student's t -test; GAPDH was used as a loading control for cell lysis; CD9 was used as a loading control for sEV lysis).
- F Establishment of LSD1 knockout (KO) MGC-803 cell line. Con indicates MGC-803 cells, while KO indicates LSD1 KO MGC-803 cells.
- G, H Transmission electron microscopy images (G) and the size distribution (H) of sEVs from MGC-803 and LSD1 KO MGC-803 cells. Scale bar = 100 nm.
- I Expression levels of LSD1, CD63, CD9, TSG101, and calnexin in sEVs from MGC-803 and LSD1 KO MGC-803 cells. sEVs were extracted using two different extraction methods (ultracentrifugation (UC) and commercial kit). Calnexin is an sEV negative marker. UC, sEVs isolated using the ultracentrifugation method; Kit, sEVs isolated using the commercial kit.
- J Expression levels of LSD1, CD63, and CD9 in sEVs with indicated treatment.

Source data are available online for this figure.

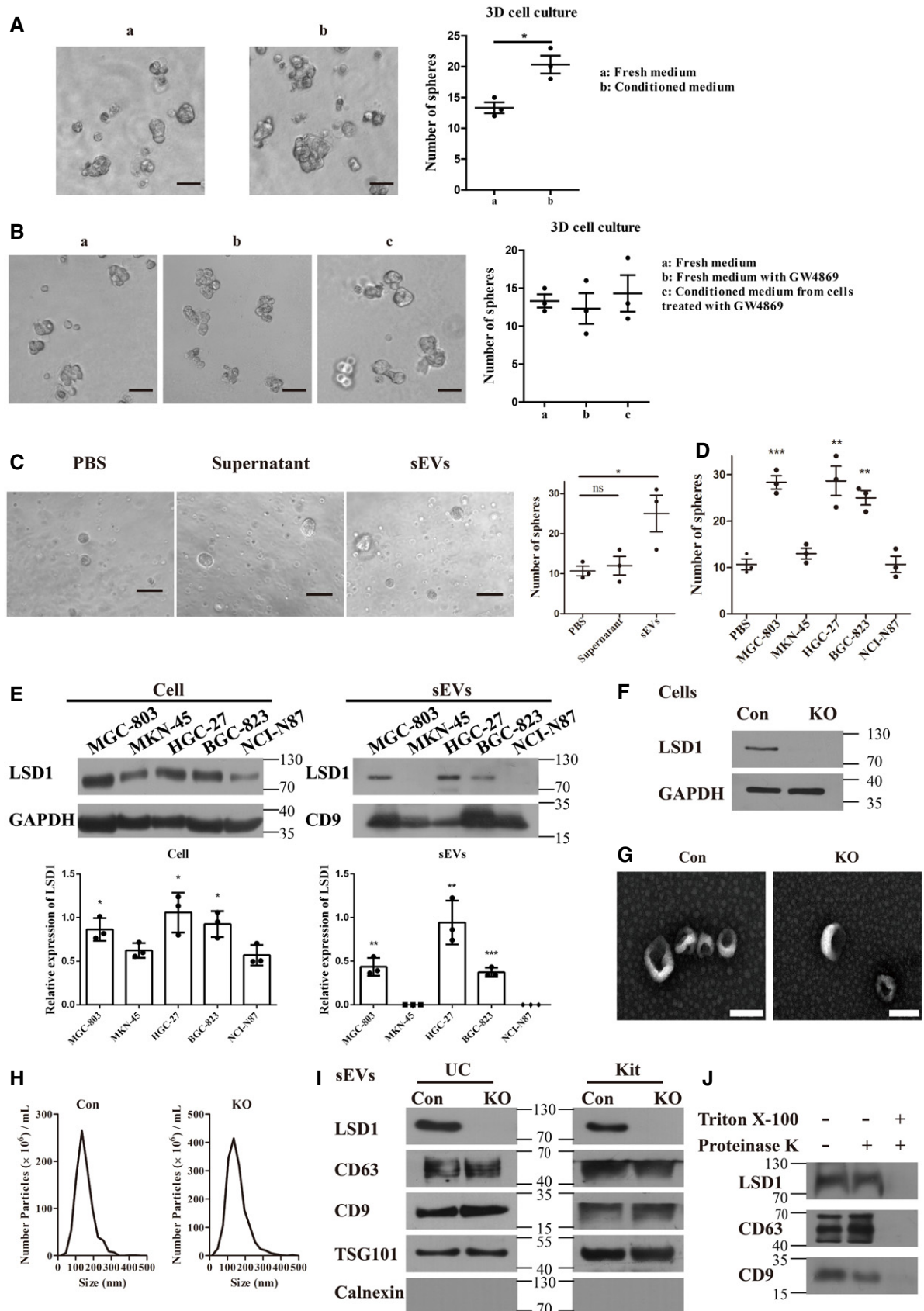


Figure 1.

SPOCTOPUS (Viklund *et al*, 2008). However, LSD1 is localized to the nucleus (Shi *et al*, 2004). The correlation between sEVs and LSD1 is unclear. In this study, the expression of LSD1 in sEVs derived from MGC-803, MKN-45, HGC-27, BGC-823, and NCI-N87 cell lines was examined (Fig 1E; right panel). sEVs derived from MGC-803, HGC-27, and BGC-823 cells exhibited higher levels of LSD1 than those derived from other cell lines. This was consistent with the LSD1 expression levels in the cells. Consistently, sEVs derived from MGC-803, HGC-27, and BGC-823 cells exhibited enhanced ability to promote sphere formation in the recipient cells (Fig 1D). In addition to promoting sphere formation in the recipient cells, sEVs dose-dependently enhanced the levels of LSD1 in the recipient cells (Fig EV1C–D). Next, the role of the sEV cargo LSD1 in promoting the stemness of gastric cancer cells was examined.

sEVs from MGC-803 and *LSD1* knockout (KO) MGC-803 cells (Fig 1F) were subjected to transmission electron microscopy (TEM). The size distribution was monitored using NanoSight particle tracking analysis (NTA) for quality control (Fig 1G–H). Additionally, the protein content in the sEVs was analyzed using mass spectrometry to examine the effect of *LSD1* KO on sEV contents. As shown in Fig EV1E, the distribution of proteins with different masses was not significantly different between sEVs derived from MGC-803 and those derived from *LSD1* KO MGC-803 cells. As shown in Fig 1I, the analysis of LSD1 levels revealed that LSD1 was enriched in sEVs derived from MGC-803 but not in those derived from *LSD1* KO MGC-803 cells, no matter the sEVs isolated by ultracentrifugation or commercial kits. Meanwhile, the levels of sEV markers (CD63, TSG101, and CD9) were constant and the sEV negative marker calnexin was not detected. To further confirm the presence of LSD1 in sEVs, the MGC-803 cell-derived sEVs were treated with proteinase K, Triton X-100, or their combination. As shown in Fig 1J, LSD1 was not detected upon treatment with the combination of proteinase K and Triton X-100. This is because Triton X-100 damages the structure of sEVs, which allows proteinase K penetration and consequently the digestion of proteins in sEVs. Treatment with proteinase K did not affect the LSD1 levels as proteinase K could not penetrate and damage the proteins in sEVs. This indicated that LSD1 was within the sEVs.

These results demonstrate that sEVs secreted from gastric cancer cells promote sphere formation and that LSD1 is secreted through sEVs. However, the delivery of sEVs harboring LSD1 to the recipient cells must be further clarified.

LSD1-containing sEVs can deliver LSD1 to target cells

The ability of sEVs to fuse with recipient cells was examined. As shown in Fig 2A, sEVs (stained with PKH26; red) from MGC-803 (Con sEVs) and *LSD1* KO MGC-803 cells (KO sEVs) fused with recipient MGC-803 and MKN-45 cells (cell membrane was stained with Dio; green and nuclei were stained with 4',6-diamidino-2-phenylindole (DAPI)). Next, the *LSD1* KO MGC-803 and MKN-45 cells were incubated with Con and KO sEVs. LSD1 was detected only in *LSD1* KO MGC-803 and MKN-45 cells treated with Con sEVs but not in those treated with KO sEVs (Fig 2B). These results demonstrate that the nuclear protein LSD1 can be delivered into recipient gastric cancer cells through sEVs.

LSD1 promotes stemness by facilitating the accumulation of SOX2

Next, the role of LSD1 in gastric cancer was examined. The expression of LSD1 in gastric cancer tissues was analyzed using The Cancer Genome Atlas data from UALCAN (<http://ualcan.path.uab.edu/index.html>) (Chandrashekar *et al*, 2017). As shown in Fig 3A, the expression of LSD1 in gastric cancer tissues was upregulated when compared with that in the adjacent normal tissues. Furthermore, the expression of LSD1 in clinical specimens was analyzed using the data from Gene Expression Profiling Interactive Analysis (GEPIA) (<http://gepia.cancer-pku.cn/>) (Tang *et al*, 2017). As shown in Fig 3B, the expression of LSD1 in the gastric cancer tissues was upregulated when compared with that in the adjacent non-cancerous tissues. The overall survival analysis of data from GEPIA also confirmed that the expression of LSD1 in gastric cancer tissue was associated with poor prognosis (Fig 3C). These findings indicate that the enhanced expression of LSD1 in gastric cancer tissues is associated with poor clinical outcomes. However, the role of LSD1 in poor prognosis of gastric cancer is unknown.

Cancer stem cells, which are a small subgroup of cells capable of self-renewal and differentiation (Clarke *et al*, 2006), contribute to tumor initiation, progression, therapeutic resistance, and tumor recurrence (Tanase *et al*, 2014). Hence, gastric CSCs (GCSCs) have piqued the interest of the scientific community. Some GCSC candidate markers are reported to be potential therapeutic targets for gastric cancer (Singh, 2013). Therefore, this study examined the role of LSD1 in gastric cancer cell self-renewal ability and chemoresistance. The results of the *in vitro* limiting dilution assays (Fig 3D) suggested that *LSD1* KO significantly inhibited the self-renewal of gastric cancer cells. Additionally, the sphere number and size of MGC-803 cells were higher than those of *LSD1* KO MGC-803 cells (Fig 3E). Meanwhile, *LSD1* KO downregulated the expression of stemness markers, including OCT4, SOX2, Nanog, and CD44, which are core transcription factors that promote self-renewal in the tumor cells (Fig 3F). The role of LSD1 in gastric cancer cell stemness was further evaluated by rescuing LSD1 expression in *LSD1* KO MGC-803 cells and treating MGC-803 cells with the LSD1 inhibitor GSK-LSD1. As shown in Fig EV2A–B, rescuing LSD1 expression effectively restored the sphere formation ability of *LSD1* KO MGC-803 cells, and treatment with GSK-LSD1 significantly attenuated the sphere formation ability of MGC-803 cells. These findings suggest that LSD1 is required for the self-renewal of gastric cancer cells and that the inhibition of LSD1 suppresses the stemness of gastric cancer cells. Next, the mechanism underlying LSD1-mediated regulation of gastric cancer cell stemness was examined.

In this study, *LSD1* KO decreased the levels of stemness markers. The correlation between LSD1 and stemness markers was examined using the data from GEPIA (Tang *et al*, 2017). LSD1 was not significantly correlated with OCT4, Nanog, and CD44 (Fig EV2C). However, LSD1 was significantly correlated with SOX2 ($R = 0.21$, $P < 0.0001$) in gastric cancer (Fig 3G). LSD1 is reported to demethylate SOX2 in ovarian cancer (Zhang *et al*, 2018). Thus, the regulatory effect of LSD1 on SOX2 in gastric cancer was investigated. Immunohistochemical analysis was performed on 172 pairs of gastric cancer tissues and adjacent non-cancerous tissues. As shown in Fig EV2D–F, the expression levels of LSD1 and SOX2 were

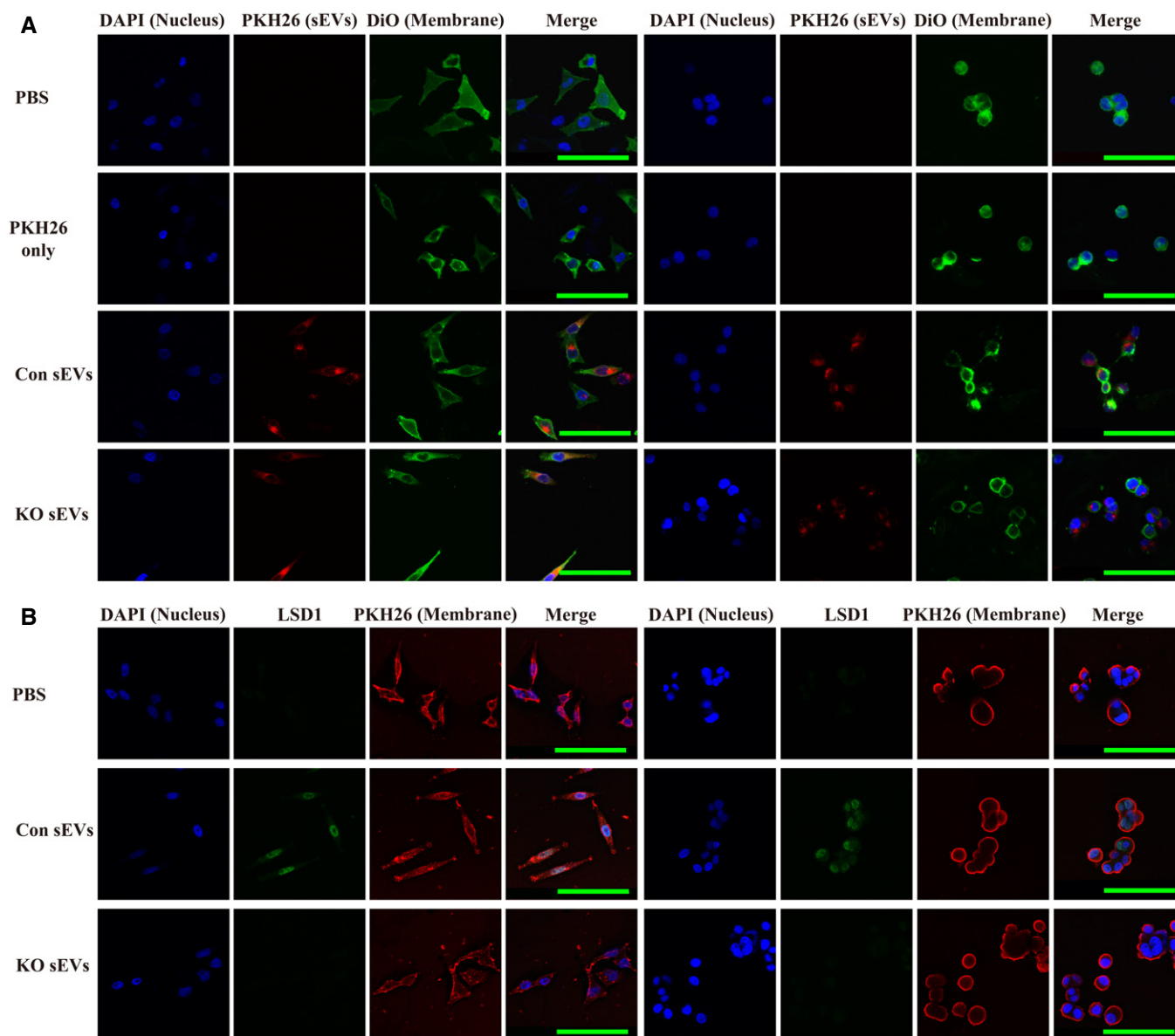


Figure 2. LSD1-containing small extracellular vesicles (sEVs) fuse to the recipient cell and deliver LSD1.

A Confocal microscopy image analysis of sEV fusion to MGC-803 cells. The MGC-803 (left side) and MKN-45 (right side) cells were treated with sEVs derived from MGC-803 cells (Con sEVs) or *LSD1* knockout (KO) MGC-803 cells (KO sEVs) and stained with PKH26 for 12 h. Additionally, the cell membrane was stained with Dio, while the nuclei were stained with 4',6-diamidino-2-phenylindole (DAPI). Scale bar = 100 μ m.

B Immunofluorescence confocal microscopy analysis of LSD1 (green) in *LSD1* KO MGC-803 cells (left panel) and *LSD1* KO MKN-45 cells (right panel) incubated with 20 μ g/ml Con sEVs and KO sEVs for 12 h. The cell membrane was stained with PKH26, while the nuclei were stained with DAPI. Scale bar = 100 μ m.

upregulated in gastric cancer tissues. Additionally, the expression of LSD1 was significantly and positively correlated with that of SOX2 ($R = 0.352$; $P < 0.001$) in gastric cancer specimens (Fig 3H).

Lysine-specific demethylase 1 demethylates lysine on SOX2, which leads to the deubiquitination and stabilization of SOX2 in CSCs (Zhang *et al*, 2013; Zhang *et al*, 2018; Zhang *et al*, 2019). Hence, the ability of LSD1 to stabilize SOX2 in gastric cancer was examined. The mRNA level of *SOX2* in MGC-803 and *LSD1* KO MGC-803 cells was examined. As shown in Fig 3I, *LSD1* KO did not

affect the *SOX2* mRNA level. Next, the MGC-803 and *LSD1* KO MGC-803 cells were treated with cycloheximide to inhibit mRNA translation. LSD1 increased the half-life of SOX2 (Fig 3J–K), which suggested that LSD1 stabilizes SOX2 in gastric cancer (Fig 3J–K). Furthermore, the MGC-803 and *LSD1* KO MGC-803 cells were subjected to immunoprecipitation assay using anti-SOX2 antibodies to examine the effect of *LSD1* KO on the levels of Kme1/2 (Fig 3L). Additionally, the anti-Kme1/2 antibody was used as a bait for SOX2 (Fig 3M). *LSD1* KO promoted the methylation of SOX2 (Fig 3L–M).

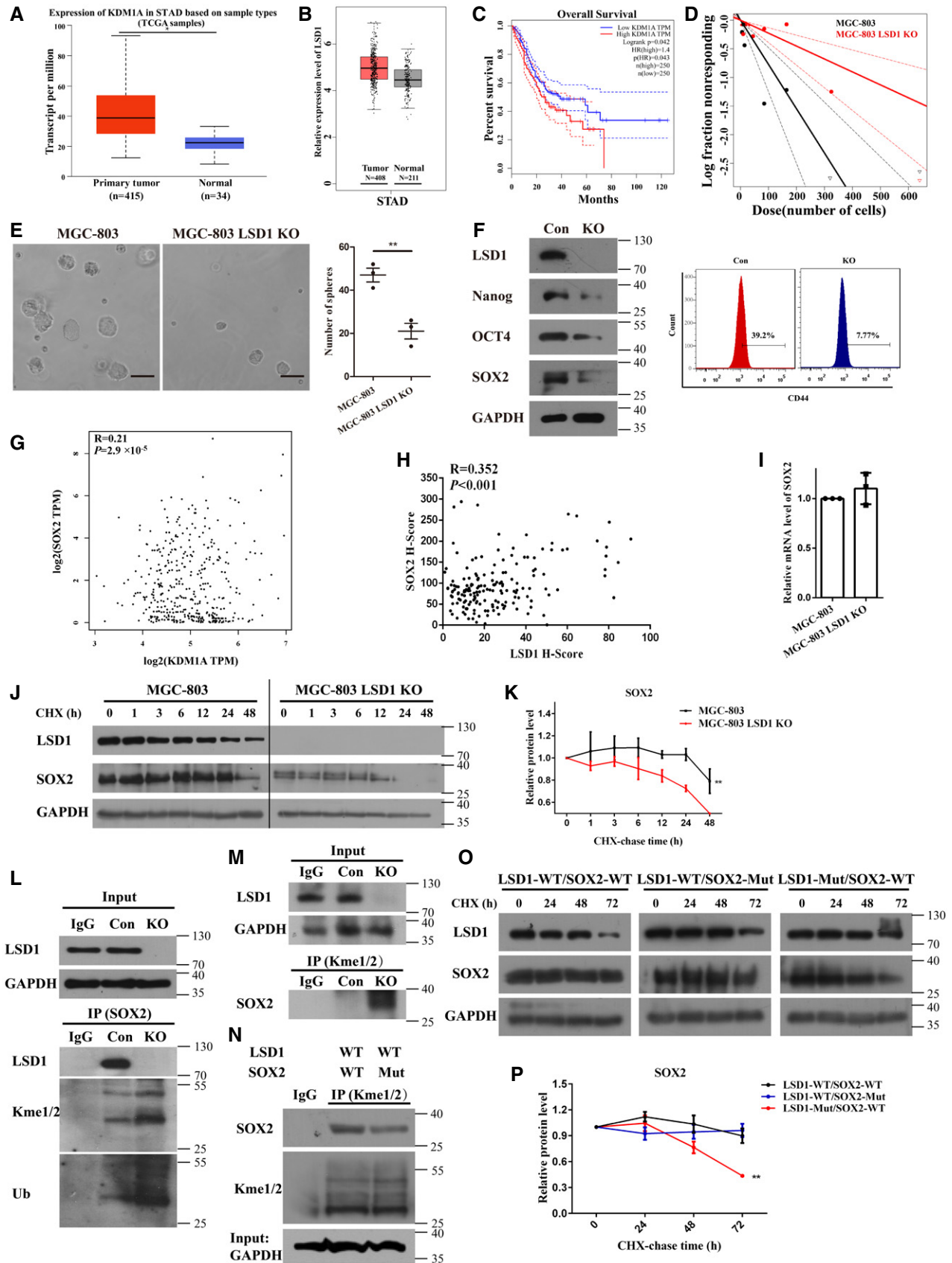


Figure 3.

Figure 3. LSD1 facilitates stemness and promotes the accumulation of SOX2.

- A Expression level of LSD1 (KDM1A) in gastric cancer and non-cancerous tissues from UALCAN datasets (STAD, stomach adenocarcinoma; central band, boxes, and whiskers of the boxplot represent the median, first quartile, third quartile, minimum, and maximum values, respectively).
- B Expression level of LSD1 (KDM1A) in gastric cancer or non-cancerous tissues from Gene Expression Profiling Interactive Analysis (GEPIA) datasets (central band, boxes, and whiskers of the boxplot represent the median, first quartile, third quartile, minimum, and maximum values, respectively).
- C Overall survival analysis using GEPIA datasets (log-rank test; the solid line represents the survival curve, while the dashed line represents the 95% confidence interval).
- D *In vitro* limiting dilution assay with MGC-803 and *LSD1* knockout (KO) MGC-803 cells (the solid line represents the sphere formation ability curve, while the dashed line represents the 95% confidence interval).
- E Sphere formation assay results of MGC-803 and *LSD1* KO MGC-803 cells. Scale bar = 100 μm ($n = 3$ biological replicates; mean \pm standard error mean (SEM); $**P = 0.0058$; two-tailed unpaired Student's *t*-test).
- F Expression levels of LSD1, Nanog, OCT4, SOX2, and CD44 in *LSD1* KO MGC-803 cells.
- G Correlation between *LSD1* and *SOX2* mRNA levels analyzed using the GEPIA dataset (Pearson's test).
- H Correlation between *LSD1* and *SOX2* in 172 gastric cancer tissues (Pearson's test).
- I The mRNA levels of *SOX2* in different cells were detected using quantitative real-time polymerase chain reaction ($n = 3$ biological replicates; mean \pm SEM).
- J Stability of *SOX2* in MGC-803 and *LSD1* KO MGC-803 cells treated with cycloheximide (20 μM) at the indicated times.
- K Relative intensity of *SOX2* in (J) ($n = 3$ biological replicates, mean \pm SEM).
- L Immunoprecipitation of Kme1/2 and ubiquitin (Ub) with *SOX2* in the presence or absence of *LSD1*. The cells were treated with MG132 (10 μM) for 8 h before analysis.
- M Reverse immunoprecipitation of Kme1/2 on *SOX2*.
- N Immunoprecipitation of Kme1/2 on *SOX2* (WT indicates HEK293T cells co-transfected with *LSD1*-WT and *SOX2*-WT; Mut indicates HEK293T cells co-transfected with *LSD1*-WT and *SOX2*-Mut; WT, wild type; Mut, mutant).
- O Stability of *SOX2* in HEK293T cells co-transfected with different plasmids (WT, wild type; *SOX2*-Mut, K42R, and K117R mutations; *LSD1*-Mut: K661A mutation).
- P Relative intensity of *SOX2* in (O) ($n = 3$ biological replicates; mean \pm SEM; $**P = 0.0055$; two-tailed unpaired Student's *t*-test).

Source data are available online for this figure.

Previous studies have reported that LSD1 demethylates K42 and K117 of SOX2 to inhibit proteolysis (Zhang *et al*, 2018; Zhang *et al*, 2019). In this study, K42R and K117R mutants of SOX2 were generated to further confirm the regulatory effect of LSD1 on SOX2 methylation in gastric cancer cells. The HEK293T cells were co-transfected with *LSD1*-wild type (WT) and *SOX2*-WT or *LSD1*-WT and *SOX2* mutant (Mut). The results of the Kme1/2 immunoprecipitation assay (Fig 3N) revealed that K42R and K117R mutations significantly decreased the lysine methylation of SOX2. Compared with that in HEK293T cells co-transfected with *LSD1*-Mut and *SOX2*-WT, *SOX2* stability was significantly higher in cells co-transfected with *LSD1*-WT and *SOX2*-WT or *LSD1*-WT and *SOX2*-Mut (Fig 3O–P). These results suggest that *LSD1*-mediated demethylation or *SOX2* mutations enhanced the stability of SOX2. However, the stability of SOX2 decreased upon mutation of *LSD1*. In summary, *LSD1* functions as a demethylase to remove the methyl groups on the lysine residues of SOX2 and consequently prevents the methylation-dependent proteolysis of SOX2. However, further studies are needed to confirm this finding.

LSD1-containing sEVs promote gastric cancer cell stemness

Next, the ability of *LSD1* delivered by sEVs to promote the stemness of recipient cells was examined. The MGC-803 and MKN-45 cells were incubated with Con and KO sEVs and subjected to sphere formation assay. As shown in Fig 4A, Con sEV-treated cells exhibited enhanced sphere formation ability. Furthermore, the results of the limited dilution assay also demonstrated that Con sEVs increased the frequency of gastric cancer cell sphere formation (Fig 4B). Meanwhile, Con sEV-treated cells exhibited upregulated expression levels of *LSD1*, *OCT4*, *SOX2*, and *CD44* when compared with control cells. In contrast, the expression levels of *LSD1*, *OCT4*, *SOX2*, and *CD44* were similar between KO sEV-treated and control cells (Fig 4C–E). This indicated that sEVs from gastric cancer cells, which exhibit upregulated *LSD1* expression, may promote the stemness of recipient gastric cancer cells. Next, the MGC-803 and MKN-45 cells were treated with sEVs from HEK293T cells, WT-*LSD1*-overexpressing HEK293T cells, and *LSD1* K661A mutant (*LSD1* K661A)-overexpressing HEK293T cells (Fig EV3). sEVs derived from

Figure 4. LSD1-containing small extracellular vesicles (sEVs) promote cancer cell stemness *in vitro*.

- A Sphere formation assay of MGC-803 and MKN-45 cells incubated with 20 $\mu\text{g}/\text{ml}$ sEVs from MGC-803 or *LSD1* knockout (KO) MGC-803 cells for 7 days ($n = 3$ biological replicates; mean \pm standard error of mean (SEM); $**P = 0.0090$ (MGC-803) and $**P = 0.0012$ (MKN-45); two-tailed unpaired Student's *t*-test; scale bar = 100 μm).
- B *In vitro* limiting dilution assays performed using MGC-803 (upper panel) and MKN-45 (bottom panel) cells incubated with 20 $\mu\text{g}/\text{ml}$ sEVs from MGC-803 or *LSD1* KO MGC-803 cells for 14 days (the solid line represents the sphere formation ability curve, while the dashed line represents the 95% confidence interval. The circles and triangles represent data from different groups).
- C Expression levels of *LSD1*, *OCT4*, and *SOX2* in MGC-803 and MKN-45 cells incubated with 20 $\mu\text{g}/\text{ml}$ sEVs from MGC-803 or *LSD1* KO MGC-803 cells for 48 h.
- D Quantification of the results of (C) ($n = 3$ biological replicates; mean \pm SEM; $*P = 0.0385$ (*LSD1*), $*P = 0.0160$ (*OCT4*), and $***P = 0.0006$ (*SOX2*) for MGC-803; $*P = 0.0299$ (*LSD1*), $*P = 0.0147$ (*OCT4*), and $*P = 0.0258$ (*SOX2*) for MKN-45; two-tailed unpaired Student's *t*-test).
- E Expression level of *CD44* in MGC-803 and MKN-45 cells incubated with 20 $\mu\text{g}/\text{ml}$ sEVs from MGC-803 or *LSD1* KO MGC-803 cells for 48 h.
- F Sphere formation assay results of MGC-803 (upper panel) and MKN-45 (bottom panel) cells incubated with 20 $\mu\text{g}/\text{ml}$ sEVs from HEK293T cells (left panel), WT-*LSD1* sEVs (middle panel), and *LSD1* K661A sEVs (right panel) for 7 days. Scale bar = 100 μm ($n = 3$ biological replicates; mean \pm SEM; $**P = 0.0021$ (MGC-803) and $**P = 0.0020$ (MKN-45); two-tailed unpaired Student's *t*-test).

Source data are available online for this figure.

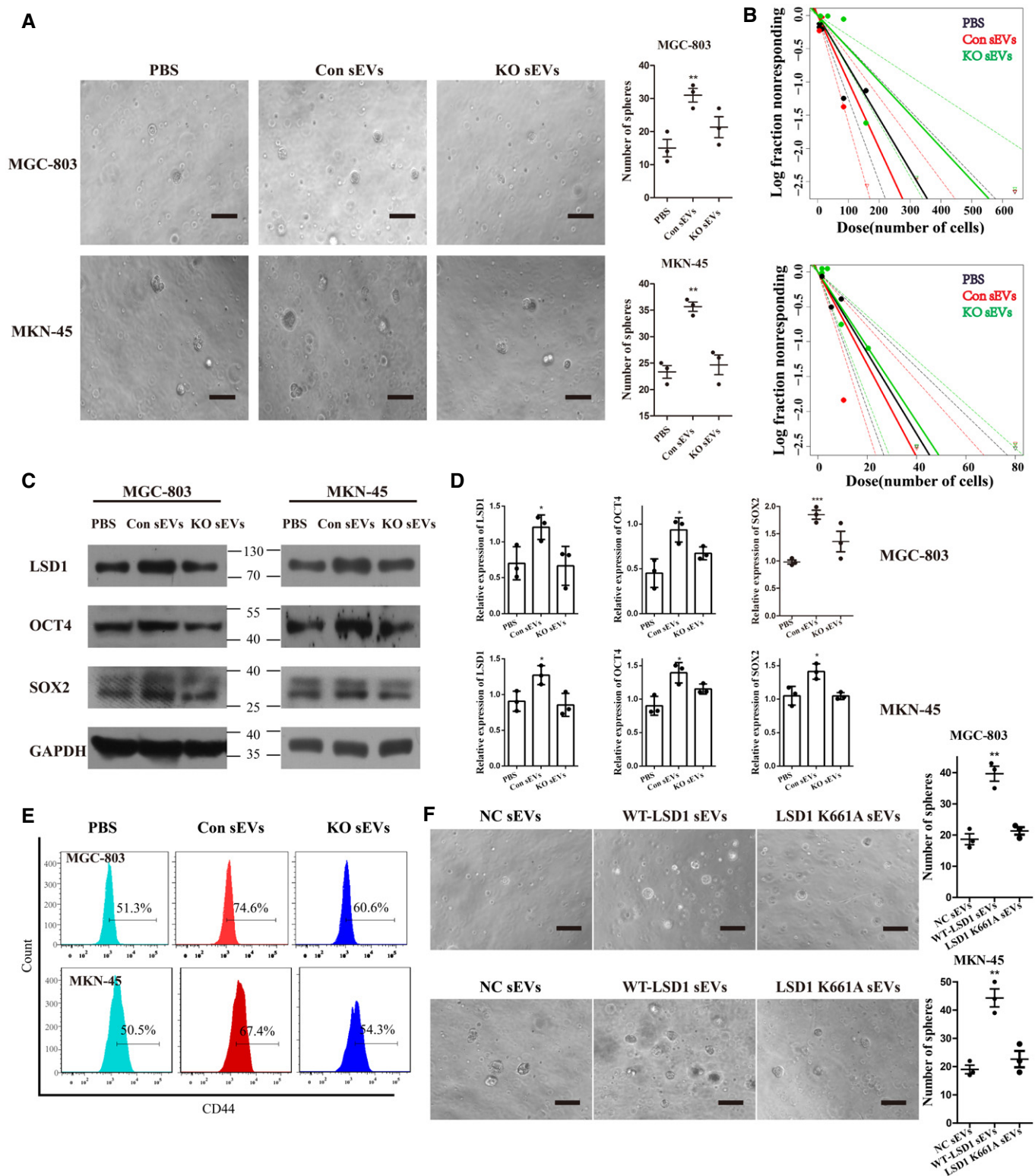


Figure 4.

WT-LSD1-overexpressing HEK29T cells (WT-LSD1 sEVs) but not those derived from LSD1 K661A-overexpressing HEK293T cells promoted sphere formation in the MGC-803 and MKN-45 cells

(Fig 4F). These results suggest that in addition to LSD1 in the cells, sEV-delivered LSD1 can promote the stemness of gastric cancer cells *in vitro*.

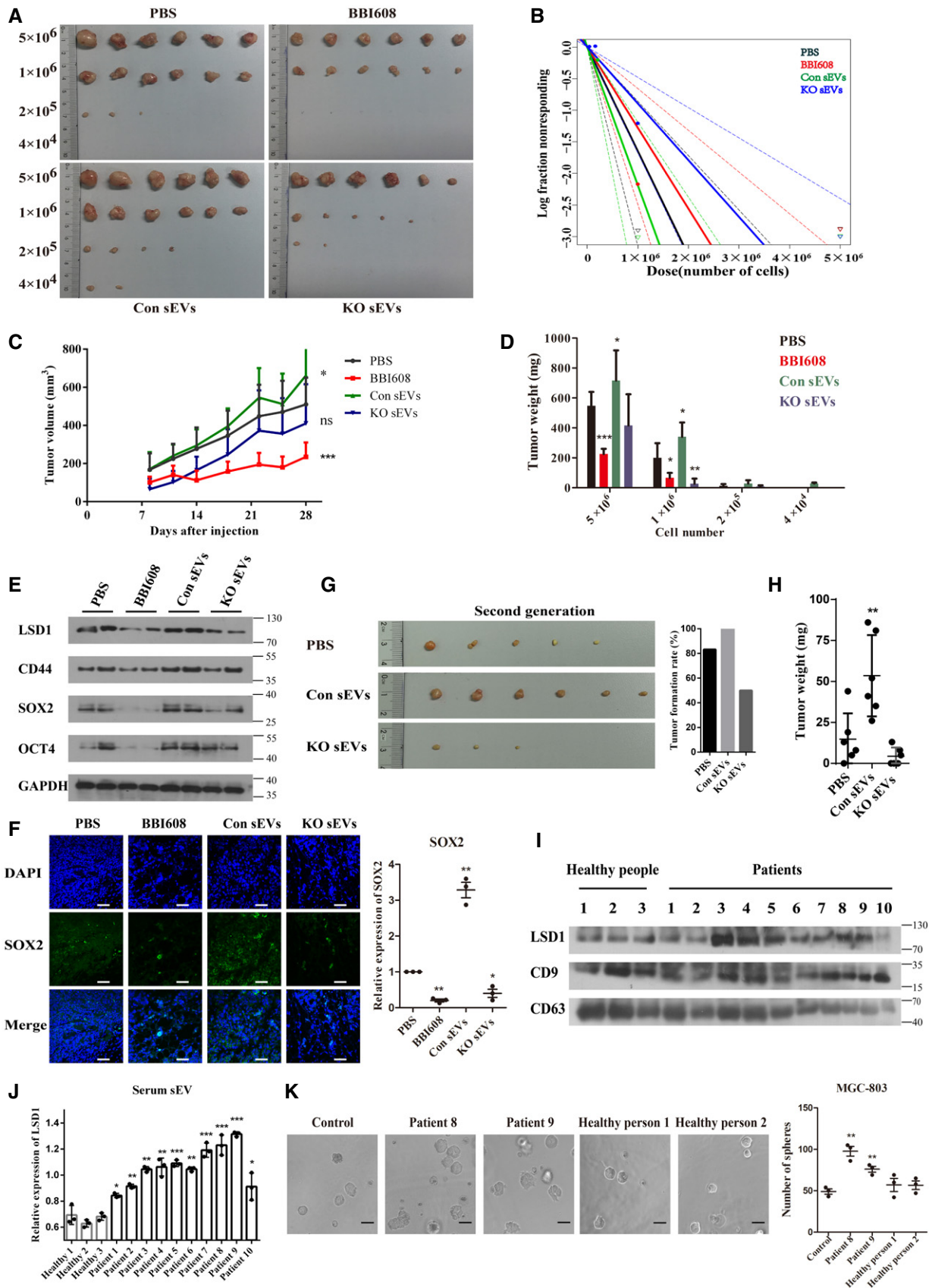


Figure 5.

Figure 5. LSD1-containing small extracellular vesicles (sEVs) promote gastric cancer cell stemness *in vivo* and clinical samples.

- A, B *In vivo* limiting dilution assay results of MGC-803 cells treated with phosphate-buffered saline, BBI608, sEVs from control cells (Con sEVs), and sEVs from *LSD1* knockout (KO) cells (KO sEVs) as indicated for 28 days in BALB/c-nu mice. Representative images of tumors excised from the mice (A) and the frequency of tumor formation (B) are shown (the solid line represents the sphere formation ability curve, while the dashed line represents the 95% confidence interval. The circles and triangles represent data from different groups).
- C Tumor volume of each group subjected to *in vivo* limiting dilution assay with 5×10^6 cells with indicated treatment ($n = 6$ biological replicates; mean \pm standard error of mean (SEM), $*P = 0.0441$ and $***P = 0.0002$; two-tailed unpaired Student's *t*-test).
- D Tumor weight of each group subjected to *in vivo* limiting dilution assay ($n = 6$ biological replicates; mean \pm SEM; $***P < 0.0001$, $*P = 0.0285$, $*P = 0.0162$, $*P = 0.0498$, and $*P = 0.0049$; two-tailed unpaired Student's *t*-test).
- E Expression levels of *LSD1*, *CD44*, *SOX2*, and *OCT4* in tumor tissues subjected to *in vivo* limiting dilution assay performed with 5×10^6 cells.
- F Immunofluorescence image and quantification of the expression of *SOX2* in tumor tissues subjected to *in vivo* limiting dilution assay. Scale bar = $50 \mu\text{m}$ ($n = 3$ biological replicates; mean \pm SEM; $**P = 0.0024$, $**P = 0.0088$, and $*P = 0.0342$; two-tailed unpaired Student's *t*-test).
- G Representative images of second-generation tumors (left) and the tumor formation rate (right) in each group.
- H Second-generation tumor weight in each group ($n = 6$ biological replicates; mean \pm SEM; $*P = 0.0091$; two-tailed unpaired Student's *t*-test).
- I, J Expression levels of *LSD1* in sEVs isolated from the plasma. *CD9* and *CD63* were used as markers of sEVs. *CD9* was used as a loading control for sEV lysis ($n = 3$ biological replicates; mean \pm SEM; $*P = 0.0256$ (patient 1), $**P = 0.0068$ (patient 2), $**P = 0.0013$ (patient 3), $**P = 0.0031$ (patient 4), $***P = 0.0009$ (patient 5), $**P = 0.0012$ (patient 6), $***P = 0.0007$ (patient 7), $***P = 0.0010$ (patient 8), $***P = 0.0001$ (patient 9), and $*P = 0.0461$ (patient 10); two-tailed unpaired Student's *t*-test).
- K Sphere formation assay results of MGC-803 cells treated with sEVs as indicated for 7 days. Scale bar = $100 \mu\text{m}$ ($n = 3$ biological replicates; mean \pm SEM; $**P = 0.0019$ and $**P = 0.0050$; two-tailed unpaired Student's *t*-test).

Source data are available online for this figure.

The findings of *in vitro* studies were verified *in vivo*. The results of the *in vivo* limiting dilution assay revealed that Con sEVs promoted the tumor formation ability of MGC-803 cells. In contrast, KO sEVs and BBI608, which inhibits stemness by selective inhibiting *STAT3* (Li *et al.*, 2015), decreased the tumor formation ability of MGC-803 cells (Fig 5A–B). In contrast to KO sEVs and BBI608, Con sEVs enhanced tumor volume and weight (Fig 5C–D). After four weeks, the mice were sacrificed and the tumor was excised. The expression of stemness markers was examined in the tumor. As shown in Fig 5E, Con sEVs upregulated the expression of *SOX2*, which suggested that it increased tumor self-renewal capacity. Moreover, the expression of *CD44* and *OCT4*, which are well-known transcription complexes, was upregulated in the cancer tissues derived from Con sEV-treated mice. Meanwhile, the expression levels of *SOX2*, *OCT4*, and *CD44* were downregulated in the KO sEV-treated and BBI608-treated groups, which was consistent with the phenotype *in vivo*. Immunofluorescence analysis further verified the regulatory effect of *LSD1* on *SOX2* *in vivo* (Fig 5F). Next, the tumor formation rate was investigated using a second-generation tumor xenograft model. As shown in Fig 5G, *LSD1* sEVs but not KO sEVs promoted second-generation tumor formation. Meanwhile, Con sEVs significantly increased the second-generation tumor weight, which further demonstrated that *LSD1*-containing sEVs promoted gastric cancer cell stemness *in vivo* (Fig 5H).

The clinical significance of *LSD1*-containing sEVs was examined. sEVs from the plasma samples of 10 patients with gastric cancer who did not undergo chemotherapy and three healthy subjects were isolated using differential ultracentrifugation. The sEVs were subjected to TEM and NTA (Fig EV4A–B) for quality control. Additionally, one sample of sEVs was chosen to verify the localization of *LSD1*. Treatment with proteinase K and Triton X-100 revealed that *LSD1* was a component of the sEV cargo in the plasma samples (Fig EV4C). As shown in Fig 5I–J, the amount of *LSD1* in sEVs isolated from the plasma samples of patients with gastric cancer was higher than that from the plasma samples of healthy subjects. Moreover, a sphere formation assay was performed with $20 \mu\text{g/ml}$ sEVs. sEVs derived from the plasma of patients with gastric cancer but not those derived from the plasma of healthy individuals promote sphere formation in MGC-803 cells (Fig 5K), which further confirmed the importance of sEVs in delivering *LSD1* in human subjects. To study the clinical relevance of sEVs-*LSD1*, the expression of *SOX2* in the tissues of 10 patients that were used to isolate sEVs was investigated using IHC. As shown in Fig EV4D–E, the amount of *LSD1* in sEVs was positively correlated with the level of *SOX2* in tissues. This indicates that sEVs-*LSD1* is closely related to the stemness of gastric cancer tissues. Thus, sEV-delivered *LSD1* plays a vital role in sEV-induced gastric cancer cell stemness *in vivo* and clinical settings.

Figure 6. LSD1-containing small extracellular vesicles (sEVs) induce oxaliplatin resistance in gastric cancer cells.

- A–D Proliferation assay results of MGC-803 (A), MKN-45 (B), NCI-N87 (C), and *LSD1* knockout (KO) MGC-803 (D) cells treated with oxaliplatin along with indicated treatments ($n = 3$ biological replicates, mean \pm standard error of mean (SEM); $*P = 0.0204$ (MGC-803), $*P = 0.0498$ (MKN-45), $*P = 0.0473$ (NCI-N87), and $*P = 0.0019$ (*LSD1* KO MGC-803); two-tailed unpaired Student's *t*-test).
- E, F Representative images of tumors (E) and the tumor weight (F) of mice treated with oxaliplatin in the presence or absence of sEVs ($n = 3$ biological replicates; mean \pm SEM; $*P = 0.0488$; two-tailed unpaired Student's *t*-test).
- G Tumor growth rate in mice treated with oxaliplatin in the presence or absence of sEVs. Tumor growth rate was measured according to tumor volume ($n = 3$ biological replicates; mean \pm SEM; $*P = 0.0439$; two-tailed unpaired Student's *t*-test).
- H Proliferation assay results of MGC-803 cells treated with oxaliplatin in the presence or absence of sEVs from the plasma of patients with gastric cancer or healthy individuals ($n = 3$ biological replicates; mean \pm SEM; $*P = 0.0487$; two-tailed unpaired Student's *t*-test).
- I Schematic model for the shuttling of *LSD1* from parent cells to recipient cells using sEVs as vehicles. The sEV-delivered *LSD1* promotes recipient gastric cancer stemness and chemoresistance.

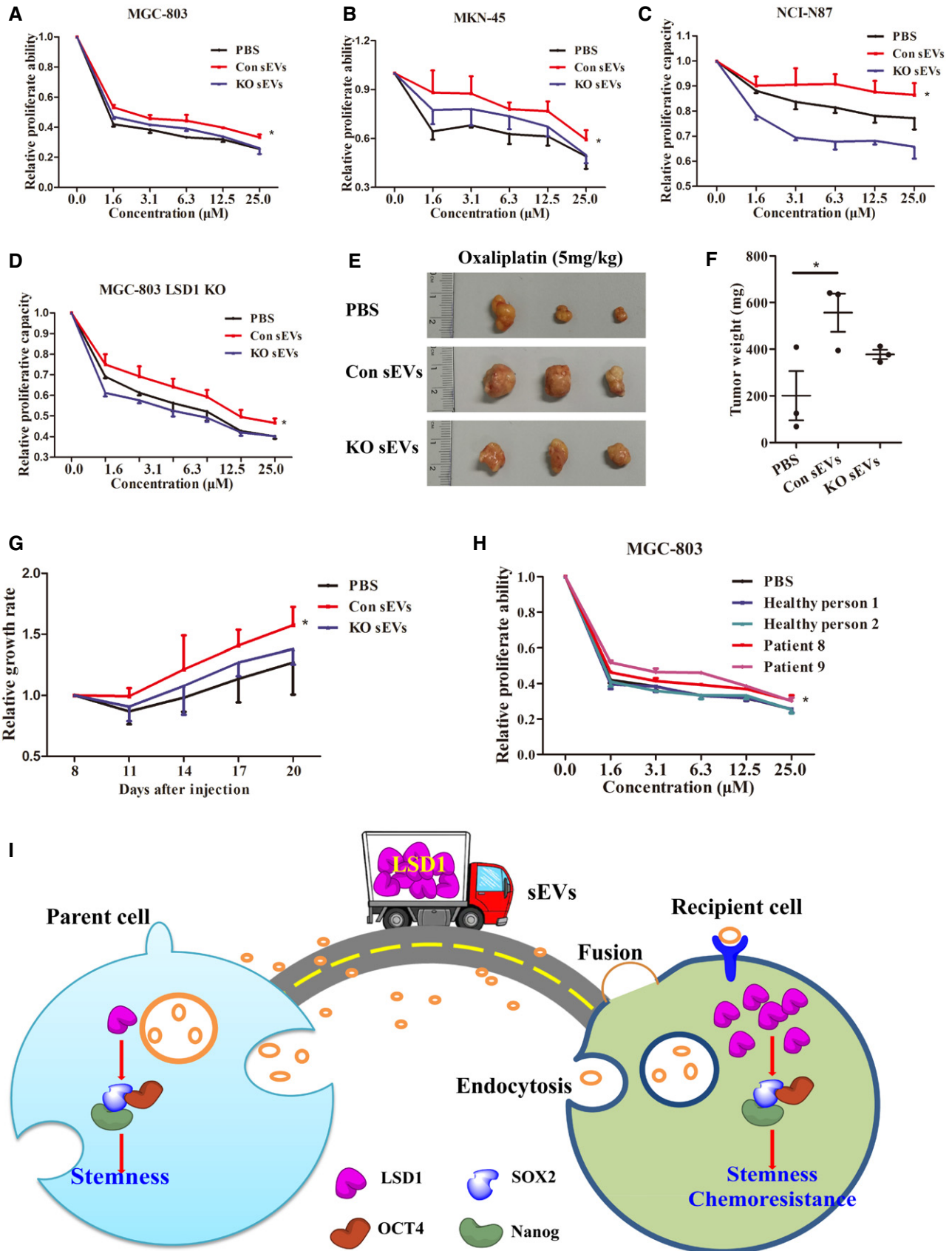


Figure 6.

LSD1-containing sEV-induced stemness mediates oxaliplatin resistance in gastric cancer cells

CSCs are associated with tumorigenicity, drug resistance, and self-renewal (Shibue & Weinberg, 2017). Therefore, CSCs are considered to be the main cause of chemoresistance (Brabletz, 2012). Oxaliplatin, a third-generation platinum-based anticancer drug, is used both as adjuvant and palliative agents for gastric cancer chemotherapy. Hence, sEV-induced resistance to oxaliplatin was examined. MKN-45, NCI-N87, and *LSD1* KO MGC-803 cells were chosen as references as they exhibit decreased *LSD1* expression or do not exhibit *LSD1* expression. As shown in Fig 6A–D, Con sEVs but not KO sEVs significantly decreased oxaliplatin sensitivity in MGC-803, MKN-45, NCI-N87, and *LSD1* KO MGC-803 cells. Further *in vivo* experiments using a subcutaneous xenograft model also suggested that *LSD1*-containing sEVs decreased the sensitivity of MGC-803 cells to oxaliplatin. The Con sEV-treated group exhibited higher tumor weight than KO sEV-treated group (Fig 6E–F). Additionally, the Con sEV-treated group exhibited significantly faster tumor growth than the KO sEV-treated and phosphate-buffered saline (PBS)-treated groups (Fig 6G). Next, the clinical significance of *LSD1*-containing sEVs was examined. A proliferation assay was performed using MGC-803 cells treated with oxaliplatin and sEVs derived from the plasma of patients with gastric cancer and healthy individuals. As shown in Fig 5H, sEVs in the plasma from patients with gastric cancer upregulated *LSD1* expression and significantly decreased the oxaliplatin sensitivity of MGC-803 cells. However, the oxaliplatin sensitivity was not significantly different between the healthy plasma sEV-treated groups and the PBS-treated group (Fig 6H). These results indicate that *LSD1*-containing sEVs can induce oxaliplatin resistance in gastric cancer cells *in vitro* and *in vivo*.

Discussion

Globally, gastric cancer is one of the most common malignancies. However, chemotherapy for gastric cancer is associated with side effects, low response rates, and chemoresistance. Chemoresistance is a major challenge for patients with gastric cancer undergoing chemotherapy. The molecular mechanisms of chemoresistance in gastric cancer include decreased intracellular concentrations of drugs, cell stemness, and alterations in drug targets. However, there are no clinical strategies or biomarkers to predict the response to chemotherapy. Hence, there is a need to identify novel molecular mechanisms to mitigate chemoresistance or predict the response to chemotherapy (Baguley, 2010). The discovery of cancer stemness, which is the main cause for chemoresistance, has advanced our understanding of tumorigenesis and chemoresistance and may provide novel targets for cancer therapy (Shibue & Weinberg, 2017). Therefore, the mechanism underlying gastric cancer stemness must be elucidated and novel biomarkers must be identified to predict the response to chemotherapy in gastric cancer. In this study, conditioned medium of gastric cancer cells promoted sphere formation in the recipient gastric cancer cell lines. Treatment with GW4869, an inhibitor of sEVs biogenesis and release, mitigated gastric cancer cell conditioned medium-induced sphere formation in the recipient

cells. This indicated that some components in the conditioned medium may promote cancer cell stemness.

The cargos, including RNA, DNA, and proteins, of sEVs from the parent cells are delivered to the recipient cells. Hence, sEVs have a major role in cell–cell communication (Kalluri, 2016). The conditioned medium was divided into sEV fraction and non-sEV fraction. Only the sEV fraction promoted sphere formation in the recipient cells, which suggested that cargos in sEVs promote the stemness of recipient cells.

Screening of a small panel of gastric cancer cell lines and their sEVs revealed the presence of *LSD1* in sEVs. *LSD1* is a FAD-dependent demethylase that regulates embryonic development, cell differentiation, epithelial–mesenchymal transition, cell metastasis, and mitochondrial respiration in diverse cells (Wang *et al*, 2007; Sun *et al*, 2011; Hino *et al*, 2012; Zheng *et al*, 2013; Zheng *et al*, 2015; Thambyrajah *et al*, 2016; Hosseini & Minucci, 2017). However, *LSD1* was localized to the cell nucleus. *LSD1* is a potential therapeutic target for cancer. Previous studies have focused on the biological role of *LSD1* as a nuclear protein. However, the findings of this study indicated that *LSD1* can also be secreted through sEVs. This was also confirmed by analyzing the contents of the sEVs. The mechanism underlying the packaging of the nuclear protein *LSD1* into sEVs has not been elucidated. The nuclear components can be loaded into sEVs through micronuclei (MN), which can be encapsulated into multivesicular bodies (MVBs) and consequently form a part of sEVs (Yokoi *et al*, 2019). *LSD1* may be loaded into sEVs through similar mechanisms. Additionally, sEVs derived from gastric cells may fuse with target cells and deliver *LSD1* to the recipient cells. sEV-delivered *LSD1* in recipient cells promoted the stemness and chemoresistance of gastric cancer cells both *in vitro* and *in vivo*. In addition to the sEVs derived from cell lines, the sEVs isolated from the plasma of patients with gastric cancer promoted the stemness and chemoresistance of recipient cells. This novel oncogenic mechanism of *LSD1* explains the stemness and chemoresistance of gastric cancer. Thus, sEV-delivered *LSD1* may serve as a potential marker for predicting the clinical response of patients to oxaliplatin treatment.

In this study, the role of sEV-delivered *LSD1* in regulating the stemness of gastric cancer *in vivo* was examined. Interestingly, the tumor size slightly decreased in mice treated with KO sEVs. This suggests that in addition to *LSD1*, other components of sEVs may suppress the growth of cancer cells. *LSD1* was reported to promote the expression of some key components of RNAi-induced silencing complex (such as DICER, AGO2, and TRBP2) (Sheng *et al*, 2018). Therefore, miRNA in sEVs from *LSD1* KO MGC-803 cells may be dysregulated, which may contribute to the proliferation of recipient cells. Additionally, Nanog is reported to be secreted from high-grade serous carcinoma cells into exosomes in effusion supernatants (Sherman-Samis *et al*, 2019). *LSD1* positively regulated Nanog in MGC-803 cells. Hence, Nanog and *LSD1*-containing sEVs may promote the stemness of recipient cells together. Additionally, *LSD1* stabilized SOX2 through demethylation in MGC-803 cells. The results of this study suggest that *LSD1* functions as a demethylase to remove the methyl groups on lysine of SOX2 and consequently prevents the methylation-dependent proteolysis of SOX2. However, further studies are needed to confirm these findings.

In summary, this study demonstrated that *LSD1* is secreted through sEVs, which can be delivered to the recipient cells and

consequently promote their stemness and chemoresistance (Fig 6I). LSD1 has been detected in some cancer cell-derived sEVs (Liang *et al*, 2013; Skogberg *et al*, 2013; He *et al*, 2015). However, this is the first study to report the function and the clinical application prospects of LSD1-containing sEVs in gastric cancer. The findings of this study provided novel insights into the role of LSD1 in gastric cancer cell stemness. Thus, LSD1 is a potential therapeutic target for cancer. Additionally, sEV-delivered LSD1 can be a potential biomarker to predict oxaliplatin response in clinical settings.

Materials and Methods

Cells and cell culture conditions

The gastric cancer cell lines MGC-803, BGC-823, NCI-N87, and HGC-27 were purchased from the Cell Bank of the Shanghai Institute of Cell Biology, Chinese Academy of Sciences. MKN-45 cells were purchased from the Shanghai Bogoo Biotechnology Company. The cells were maintained in Roswell Park Memorial Institute (RPMI) 1640 medium (BI, Israel) supplemented with 10% fetal bovine serum (BI, Israel). All cells were cultured in a humidified atmosphere at 5% CO₂ and 37°C.

The lentiviral vector containing Lenti-CAS9-sgRNA was produced and packaged by Shanghai Genechem Co. Ltd., China. The sgRNA target site for deleting *LSD1* was 5'-CCGGCCCTACTGTCTGCCT-3'. For transfection with Lenti-CAS9-sgRNA, the MGC-803 cells (5×10^4 cells/well) were seeded in 24-well plates and cultured in RPMI-1640 medium (BI, Israel) supplemented with 10% FBS (BI, Israel). The lentivirus was added to 500 μ l complete medium at a final concentration of 10^7 TU/ml. After 20 h of incubation, the lentivirus-containing medium was replaced with complete medium. At day 2 post-lentiviral transfection, the cells were incubated with 0.5 μ g/ml puromycin in culture medium for 3 days to select the stable *LSD1* KO cell line.

Western blotting

Equal amounts (20 μ g) of sEVs were resuspended in PBS and treated with 1 μ g/ml proteinase K for 20 min at 37°C or 0.1% Triton X-100 for 20 min, followed by treatment with 1 μ g/ml proteinase K for 20 min at 37°C. Untreated sEVs served as a negative control. The sEVs were mixed with the loading buffer and denatured.

The whole-cell lysates were prepared using radioimmunoprecipitation assay buffer. The lysates were mixed with the loading buffer and denatured. Next, 30 μ g of cell lysate was loaded for Western blotting.

Western blotting was performed according to the standard methods. Approximately 30 μ g of protein was subjected to sodium dodecyl sulfate-polyacrylamide gel electrophoresis (SDS-PAGE) using a 10% gel. The resolved proteins were transferred to a 0.2- μ m nitrocellulose membrane (P/N66485, Pall, USA). The membrane was blocked with 5% milk in PBS for 2 h, following by incubation with anti-LSD1 (ab129195, Abcam, England), anti-CD9 (134403, CST, USA), anti-CD63 (ab59479, Abcam, England), anti-calnexin (ab22595, Abcam, England), anti-OCT4 (ab181557, Abcam, England), anti-SOX2 (14962, CST, USA), anti-Nanog (ab21624, Abcam, England), and anti-GAPDH (AB-P-R 001, Hangzhou Goodhere Biotechnology, China) antibodies overnight at 4°C. Next, the membrane was washed with PBS containing 0.05% Tween-20 (PBST) at room temperature and incubated with

peroxidase-conjugated goat anti-rabbit IgG (ZB-2301, Zsbio, China) and peroxidase-conjugated goat anti-mouse IgG (ZB-2305, Zsbio, China) for 2 h at room temperature. The membrane was then washed with PBST at room temperature and developed using an enhanced chemiluminescence reagent (34096, Thermo Fisher, USA).

sEV isolation

The cells were cultured in serum-free medium for 36 h. The medium was centrifuged at 1,500 g for 30 min to remove cell debris, followed by centrifugation at 10,000 g for 30 min to remove large vesicles. Further, the samples were centrifuged at 100,000 g for 2 h. The supernatant was removed, and the pellet was resuspended in 2 ml of PBS. The resulting pellet was washed with PBS at 100,000 g for 2 h. The samples were centrifuged to obtain the sEVs. sEVs were resuspended in 200 μ l PBS and stored at -80°C until use. Additionally, sEVs were filtered through a 0.22- μ m filter before use. In this study, sEVs were obtained using differential ultracentrifugation unless otherwise specified. For the isolation of plasma-derived sEVs, the plasma was diluted 10 times before differential ultracentrifugation. Quantification of sEVs was performed using the bicinchoninic acid assay.

The kit used for sEV isolation was the total exosome isolation reagent (4478359, Invitrogen, USA). Briefly, the medium was collected and centrifuged at 1,500 g for 30 min to remove cell debris, followed by centrifugation at 10,000 g for 30 min to remove large vesicles. The supernatant was incubated with the exosome isolation reagent at a ratio of 3:1 (v/v) at 4°C overnight. The samples were centrifuged at 10,000 g, and the precipitate was collected (sEVs).

All sEVs in this study were obtained using differential ultracentrifugation, except those in Fig 1I, which were isolated using total exosome isolation reagent (4478359, Invitrogen, USA). The reagent was only used for verification of the presence of LSD1 in sEVs. All the sEVs in this study were filtered through 0.22- μ m membrane filters before functional experiments.

The relevant data from the experiments are submitted to the EV-TRACK knowledgebase (EV-TRACK ID: EV200198) (Van Deun *et al*, 2017).

sEV labeling

Purified sEVs were labeled using the PKH26 red fluorescent labeling kit (MINI26-1KT, Sigma, Germany), following the manufacturer's instructions. Briefly, sEVs were incubated with diluted PKH26 in a ratio of 1:1 (v/v) for 5 min. Size exclusion chromatography was performed to remove PKH26 micelles from the labeled sEVs. The PKH26-labeled sEVs (20 μ g/ml) were incubated with 1.2×10^4 target cells for 12 h. The target cell membrane was stained with Dio (C1038, Beyotime, China), while the nuclei were stained with DAPI (BS130A, Biosharp, China). PKH26-labeled sEVs were examined using a confocal microscope (Nikon, Japan).

Immunoprecipitation

Immunoprecipitation kit was purchased from Thermo Fisher Scientific (26147, Thermo Fisher Scientific, USA). The Kme1/2 or SOX2 complexes were purified from 1–2 mg of total protein using the

anti-Kme1/2 (PTM602, PTM Biolabs, China) or anti-SOX2 antibody (14962, CST, USA) coupled to protein A/G Dynabeads (26147, Thermo Fisher Scientific, USA). The protein-bead complexes were washed and eluted. The sample was then heated with loading buffer at 95–100°C for 10 min. Next, the sample was cooled to room temperature and subjected to SDS–PAGE analysis.

Immunofluorescence

The cells were cultured in a 24-well plate. The recipient cells were incubated with 20 µg/ml of sEVs or PBS for 12 h. The cells were fixed with 4% paraformaldehyde and permeabilized with 0.01% Triton X-100 for 20 min. Next, the cells were probed with anti-LSD1 (ab129195, Abcam, England) antibodies. After washing with PBS at room temperature, the cells were incubated with anti-rabbit secondary antibodies (A32723, Life, USA) for 2 h at room temperature. The samples were treated with DAPI (BS130A, Biosharp, China) for staining cell nucleus and PKH26 (MINI26-1KT, Sigma, Germany) for membrane staining. The cells were imaged using a Nikon C2 Plus confocal microscope (Nikon, Japan).

Extreme limiting dilution assay

A limiting dilution assay is an experimental technique for quantifying the proportion of biologically active components in a large population (Hu & Smyth, 2009). This assay is a type of dose-response experiment in which each culture exhibits a negative or positive response. The rate of positive and negative responses at each dose allows the determination of the frequency of biologically active components. Stem cell assays reflect cell stemness (Zhang *et al*, 2017b).

The *in vitro* limiting dilution assay was performed as previously described (Zhou *et al*, 2016). Briefly, gastric cancer cells subjected to different treatments were digested, diluted to single-cell suspensions, and plated in 96-well plates at a cell number of 1, 2, 5, 10, 20, 40, 80, 160, and 320 cells per well. Wells without spheres were counted after one week. Extreme limiting dilution assays were performed using the software available at <http://bioinf.wehi.edu.au/software/elda/> (Hu & Smyth, 2009).

Three-dimensional (3D) cell culture

Cell sphere formation experiments were performed using the 3D cell culture media (D112501, Sciobio, China). The cells in 3D cell culture medium were plated into a 96-well plate. Next, the cells were incubated with 10 µl of cell complete medium. After the medium became gelatinous, the cell culture medium was added to each well. After one week, the spheres were counted and photographed using a microscope (Nikon Ts2, Nikon, Japan).

Flow cytometric analysis

The treated cells were resuspended in PBS and incubated with the anti-CD44 antibody (555479, BD, USA) for 20 min on ice. Next, the cells were washed thrice with PBS and subjected to flow cytometric analysis using the LSRFortessa™ Cell Analyzer (Becton Dickinson, USA). Flow cytometric data were analyzed using FlowJo 7.6 software (FlowJo, USA).

Mouse tumor xenograft model

Five-week-old female BALB/c nude mice were purchased from the Jingda Laboratory Animal, Hunan, China. All animals were housed in a pathogen-free environment, and the experimental protocols were approved by the Ethics Committee of Zhengzhou University Health Science Center. The *in vivo* limiting dilution assay was performed as previously described (Zhou *et al*, 2016). Briefly, the gastric cancer cells treated with different sEVs were digested and resuspended in sterile PBS. The cells were diluted to different concentrations of (5×10^6 , 1×10^6 , 2×10^5 , and 4×10^4 per 200 µl). An aliquot (200 µl) of the cell suspension from each group was inoculated subcutaneously into mice. Tumor volume was monitored every 3 days using a digital caliper. The tumor volume was calculated as follows: tumor volume (mm^3) = length \times width² \times 0.5. The tumors were administered with sEVs (20 µg sEVs/tumor) twice a week after the tumor volume reached 100 mm^3 (1 week). On day 28, the mice were euthanized and the tumors were excised and weighed.

For experiments evaluating drug sensitivity, MGC-803 cells were used to construct a subcutaneous xenograft model. Three groups were intraperitoneally treated with oxaliplatin (5 mg/kg body-weight; dissolved in PBS) in the presence or absence of sEVs. The tumor growth rate was measured according to the tumor volume.

Second-generation tumor xenograft model

A first-generation transplanted tumor was selected for each group. The tumor was excised, equally divided into blocks based on the volume, and transplanted into mice. The tumor formation rate was determined after two weeks. After the tumor volume reached 100 mm^3 (one week), the tumor volume was quantified every 3 days using a digital caliper as follows: tumor volume (mm^3) = length \times width² \times 0.5.

CCK-8 assay

Cell proliferation was quantified using the CCK-8 method (HY-K0301, MCE, USA). The cells were seeded in 96-well plates and incubated with 10 µl CCK-8 solution for 4 h. The absorbance of the mixture at 450 nm was measured using a microplate reader (Envision, PerkinElmer, USA).

Immunohistochemistry

The specimens were fixed in 10% buffered formalin solution and embedded in paraffin wax. The serial sections (5 µm) were cut from the tissue blocks, deparaffinized in xylene, and hydrated in an alcohol series (75, 85, 95, and 100%). The tissue sections were then incubated with anti-LSD1 (ab129195; Abcam) and anti-SOX2 (14962; CST) antibodies. Further, the tissue sections were incubated with peroxidase-conjugated goat anti-rabbit Ig (ZB-2301; Zsbio, China) or peroxidase-conjugated goat anti-mouse IgG (ZB-2305; Zsbio, China) for 2 h at room temperature. Immunoreactive bands were developed using the 3,3'-diaminobenzidine kit (ZL1-9018, ZSGB-BIO, China). The sections were digitally scanned using an Aperio AT2 scanner (Leica Biosystems, Germany). The images were analyzed with Aperio Image Toolbox (Leica Biosystems,

Germany) using a pathologist-trained nuclear-, cytoplasmic-, nuclear and cytoplasmic-, and cytoplasmic-specific algorithms. Protein expression was evaluated according to the H-score system. The percentage of staining intensity was scored as 0 (no staining), 1+ (weak staining), 2+ (moderate staining), and 3+ (strong staining). The degree of expression in each sample was reported as the percentage of positive cells (0 to 100%). The final score (H-score) was then obtained by multiplying the intensity and reactivity extent values (range, 0–300).

Statistical analysis

Three independent trials were performed for each *in vitro* experiment. Pearson's correlation coefficient was used to evaluate the correlation between the groups. The differences were considered significant at $P < 0.05$, and $P < 0.01$ was considered highly significant. All statistical analyses were performed using GraphPad 6.0 or SPSS 21.0. The data were analyzed using Student's *t*-test. * $P < 0.05$, ** $P < 0.01$, *** $P < 0.001$.

Ethical approval

Gastric cancer tissues and adjacent tissues were obtained from the First Affiliated Hospital of Zhengzhou University. All human tissues were collected using protocols approved by the Ethics Committee of Zhengzhou University Health Science Center. The blood samples were collected from patients with gastric cancer at the First Affiliated Hospital of Zhengzhou University and approved by the Ethics Committee of Zhengzhou University Health Science Center.

Data availability

All data obtained and/or analyzed in this study are available from the corresponding authors upon reasonable request. The proteomics data in this publication have been deposited at the ProteomeXchange Consortium via the PRIDE (<https://www.ebi.ac.uk/pride>) (Perez-Riverol et al, 2019) partner repository (dataset identifier: PXD021511).

Expanded View for this article is available online.

Acknowledgments

This work was supported by the National Natural Science Foundation of China (No. 81602961, No. 81430085, and No. 21372206), the National Key Research Program (No. 2018YFE0195100, No. 2016YFA0501800, and No. 2017YFD0501401); Science and Technology Innovation Talents of Henan Provincial Education Department (19IRTSTHN001), Basic and Frontier Technology Research Project of Henan Province (No. 162300410119), and the Natural Science Foundation of Henan Province (No. 162300410292).

Author contributions

LJZ prepared the manuscript. LJZ, YYL, and QQF performed the experiments. LJZ performed the immunohistochemical analysis and evaluated the results with WCC, HMR, JRP, DDS, and ZYW. LJZ, LFZ, and JWW performed the *in vivo* experiments. CZ and AM critically evaluated the manuscript. YTZ and JYZ revised the manuscript. HML and YCZ designed the study and finalized the manuscript.

Conflict of interest

The authors declare that they have no conflict of interest.

References

- Amente S, Lania L, Majello B (2013) The histone LSD1 demethylase in stemness and cancer transcription programs. *Biochem Biophys Acta* 1829: 981–986
- Baguley BC (2010) Multidrug resistance in cancer. *Methods Mol Biol* 596: 1–14
- Bao L, You B, Shi S, Shan Y, Zhang Q, Yue H, Zhang J, Zhang W, Shi Y, Liu Y et al (2018) Metastasis-associated miR-23a from nasopharyngeal carcinoma-derived exosomes mediates angiogenesis by repressing a novel target gene TSGA10. *Oncogene* 37: 2873–2889
- Brabletz T (2012) EMT and MET in metastasis: where are the cancer stem cells? *Cancer Cell* 22: 699–701
- Bray F, Ferlay J, Soerjomataram I, Siegel RL, Torre LA, Jemal A (2018) Global cancer statistics 2018: GLOBOCAN estimates of incidence and mortality worldwide for 36 cancers in 185 countries. *CA Cancer J Clin* 68: 394–424
- Cao YL, Zhuang T, Xing BH, Li N, Li Q (2017) Exosomal DNMT1 mediates cisplatin resistance in ovarian cancer. *Cell Biochem Funct* 35: 296–303
- Chairoungdua A, Smith DL, Pochard P, Hull M, Caplan MJ (2010) Exosome release of beta-catenin: a novel mechanism that antagonizes Wnt signaling. *J Cell Biol* 190: 1079–1091
- Chandrashekar DS, Bashel B, Balasubramanya SAH, Creighton CJ, Ponce-Rodriguez I, Chakravarthi B, Varambally S (2017) UALCAN: a portal for facilitating tumor subgroup gene expression and survival analyses. *Neoplasia* 19: 649–658
- Chaput N, They C (2011) Exosomes: immune properties and potential clinical implementations. *Semin Immunopathol* 33: 419–440
- Chen G, Huang AC, Zhang W, Zhang G, Wu M, Xu W, Yu Z, Yang J, Wang B, Sun H et al (2018) Exosomal PD-L1 contributes to immunosuppression and is associated with anti-PD-1 response. *Nature* 560: 382–386
- Chen Y, Zeng C, Zhan Y, Wang H, Jiang X, Li W (2017) Aberrant low expression of p85alpha in stromal fibroblasts promotes breast cancer cell metastasis through exosome-mediated paracrine Wnt10b. *Oncogene* 36: 4692–4705
- Clarke MF, Dick JE, Dirks PB, Eaves CJ, Jamieson CH, Jones DL, Visvader J, Weissman IL, Wahl GM (2006) Cancer stem cells—perspectives on current status and future directions: AACR Workshop on cancer stem cells. *Cancer Res* 66: 9339–9344
- Duan Y, Qin W, Suo F, Zhai X, Guan Y, Wang X, Zheng Y, Liu H (2018) Design, synthesis and *in vitro* evaluation of stilbene derivatives as novel LSD1 inhibitors for AML therapy. *Bioorg Med Chem* 26: 6000–6014
- EL Andaloussi S, Mager I, Breakefield XO, Wood MJ (2013) Extracellular vesicles: biology and emerging therapeutic opportunities. *Nat Rev Drug Discov* 12: 347–357
- Enjoui S, Yabe R, Tsuji S, Yoshimura K, Kawasaki H, Sakurai M, Sakai Y, Takenouchi H, Yoshino S, Hazama S et al (2018) Stemness is enhanced in gastric cancer by a SET/PP2A/E2F1 axis. *Mol Cancer Res* 16: 554–563
- Faict S, Muller J, De Veirman K, De Bruyne E, Maes K, Vrancken L, Heusschen R, De Raeve H, Schots R, Vanderkerken K et al (2018) Exosomes play a role in multiple myeloma bone disease and tumor development by targeting osteoclasts and osteoblasts. *Blood Cancer J* 8: 105
- He M, Qin H, Poon TC, Sze SC, Ding X, Co NN, Ngai SM, Chan TF, Wong N (2015) Hepatocellular carcinoma-derived exosomes promote motility of

- immortalized hepatocyte through transfer of oncogenic proteins and RNAs. *Carcinogenesis* 36: 1008–1018
- Hino S, Sakamoto A, Nagaoka K, Anan K, Wang Y, Mimasu S, Umehara T, Yokoyama S, Kosai K, Nakao M (2012) FAD-dependent lysine-specific demethylase-1 regulates cellular energy expenditure. *Nat Commun* 3: 758
- Hosseini A, Minucci S (2017) A comprehensive review of lysine-specific demethylase 1 and its roles in cancer. *Epigenomics* 9: 1123–1142
- Hu Y, Smyth GK (2009) ELDA: extreme limiting dilution analysis for comparing depleted and enriched populations in stem cell and other assays. *J Immunol Methods* 347: 70–78
- Huang J, Sengupta R, Espejo AB, Lee MG, Dorsey JA, Richter M, Opravil S, Shiekhhattar R, Bedford MT, Jenuwein T et al (2007) p53 is regulated by the lysine demethylase LSD1. *Nature* 449: 105–108
- Huang T, Song C, Zheng L, Xia L, Li Y, Zhou YJMC (2019) The roles of extracellular vesicles in gastric cancer development, microenvironment, anti-cancer drug resistance, and therapy. *Mol Cancer* 18: 62
- Jiang N, Xiang L, He L, Yang G, Zheng J, Wang C, Zhang Y, Wang S, Zhou Y, Sheu T-J et al (2017) Exosomes mediate epithelium-mesenchyme crosstalk in organ development. *ACS Nano* 11: 7736–7746
- Kall L, Krogh A, Sonnhammer EL (2007) Advantages of combined transmembrane topology and signal peptide prediction—the Phobius web server. *Nucleic Acids Res* 35: W429–432
- Kalluri R (2016) The biology and function of exosomes in cancer. *J Clin Invest* 126: 1208–1215
- Kontaki H, Talianidis I (2010) Lysine methylation regulates E2F1-induced cell death. *Mol Cell* 39: 152–160
- Lee Y, El Andaloussi S, Wood MJ (2012) Exosomes and microvesicles: extracellular vesicles for genetic information transfer and gene therapy. *Hum Mol Genet* 21: R125–R134
- Lei ZJ, Wang J, Xiao HL, Guo Y, Wang T, Li Q, Liu L, Luo X, Fan LL, Lin L et al (2015) Lysine-specific demethylase 1 promotes the stemness and chemoresistance of Lgr5(+) liver cancer initiating cells by suppressing negative regulators of beta-catenin signaling. *Oncogene* 34: 3188–3198
- Li J, Sherman-Baust CA, Tsai-Turton M, Bristow RE, Roden RB, Morin PJ (2009) Claudin-containing exosomes in the peripheral circulation of women with ovarian cancer. *BMC Cancer* 9: 244
- Li Y, Rogoff HA, Keates S, Gao Y, Murikipudi S, Mikule K, Leggett D, Li W, Pardee AB, Li CJ (2015) Suppression of cancer relapse and metastasis by inhibiting cancer stemness. *Proc Natl Acad Sci* 112: 1839–1844
- Li ZH, Liu XQ, Geng PF, Suo FZ, Ma JL, Yu B, Zhao TQ, Zhou ZQ, Huang CX, Zheng YC et al (2017) Discovery of [1,2,3]Triazololo[4,5-d]pyrimidine derivatives as novel LSD1 inhibitors. *ACS Med Chem Lett* 8: 384–389
- Liang B, Peng P, Chen S, Li L, Zhang M, Cao D, Yang J, Li H, Gui T, Li X et al (2013) Characterization and proteomic analysis of ovarian cancer-derived exosomes. *J Proteomics* 80: 171–182
- Lin X, Li S, Wang YJ, Wang Y, Zhong JY, He JY, Cui XJ, Zhan JK, Liu YS (2019) Exosomal Notch3 from high glucose-stimulated endothelial cells regulates vascular smooth muscle cell calcification/aging. *Life Sci* 232: 116582
- Liu H-M, Suo F-Z, Li X-B, You Y-H, Lv C-T, Zheng C-X, Zhang G-C, Liu Y-J, Kang W-T, Zheng Y-C et al (2019) Discovery and synthesis of novel indole derivatives-containing 3-methylenedihydrofuran-2(3H)-one as irreversible LSD1 inhibitors. *Eur J Med Chem* 175: 357–372
- Ono M, Kosaka N, Tominaga N, Yoshioka Y, Takeshita F, Takahashi RU, Yoshida M, Tsuda H, Tamura K, Ochiya T (2014) Exosomes from bone marrow mesenchymal stem cells contain a microRNA that promotes dormancy in metastatic breast cancer cells. *Sci Signal* 7: ra63
- Perez-Riverol Y, Csordas A, Bai J, Bernal-Llinares M, Hewapathirana S, Kundu DJ, Inuganti A, Griss J, Mayer G, Eisenacher M et al (2019) The PRIDE database and related tools and resources in 2019: improving support for quantification data. *Nucleic Acids Res* 47: D442–D450
- Qian Z, Shen Q, Yang X, Qiu Y, Zhang W (2015) The role of extracellular vesicles: an epigenetic view of the cancer microenvironment. *Biomed Res Int* 2015: 649161
- Sheng W, LaFleur MW, Nguyen TH, Chen S, Chakravarthy A, Conway JR, Li Y, Chen H, Yang H, Hsu P-H et al (2018) LSD1 ablation stimulates anti-tumor immunity and enables checkpoint blockade. *Cell* 174: 549–563.e519
- Sherman-Samis M, Onallah H, Holth A, Reich R, Davidson B (2019) SOX2 and SOX9 are markers of clinically aggressive disease in metastatic high-grade serous carcinoma. *Gynecol Oncol* 153: 651–660
- Shi Y, Lan F, Matson C, Mulligan P, Whetstone JR, Cole PA, Casero RA, Shi Y (2004) Histone demethylation mediated by the nuclear amine oxidase homolog LSD1. *Cell* 119: 941–953
- Shibue T, Weinberg RA (2017) EMT, CSCs, and drug resistance: the mechanistic link and clinical implications. *Nat Rev Clin Oncol* 14: 611–629
- Singh R, Pochampally R, Watabe K, Lu Z, Mo YY (2014) Exosome-mediated transfer of miR-10b promotes cell invasion in breast cancer. *Mol Cancer* 13: 256
- Singh SR (2013) Gastric cancer stem cells: a novel therapeutic target. *Cancer Lett* 338: 110–119
- Skogberg G, Gudmundsdottir J, van der Post S, Sandström K, Bruhn S, Benson M, Mincheva-Nilsson L, Baranov V, Tlemo E, Ekwall O (2013) Characterization of human thymic exosomes. *PLoS One* 8: e67554
- Sun GQ, Ye P, Murai K, Lang M-F, Li S, Zhang H, Li W, Fu C, Yin J, Wang A et al (2011) miR-137 forms a regulatory loop with nuclear receptor TLX and LSD1 in neural stem cells. *Nat Commun* 2: 529
- Sun K, Peng JD, Suo FZ, Zhang T, Fu YD, Zheng YC, Liu HM (2017) Discovery of tranylcypromine analogs with an acylhydrazone substituent as LSD1 inactivators: design, synthesis and their biological evaluation. *Bioorg Med Chem Lett* 27: 5036–5039
- Takahashi T, Saikawa Y, Kitagawa Y (2013) Gastric cancer: current status of diagnosis and treatment. *Cancers* 5: 48–63
- Tanase CP, Neagu AI, Necula LG, Mambet C, Enciu AM, Calenic B, Cruceru ML, Albulescu R (2014) Cancer stem cells: involvement in pancreatic cancer pathogenesis and perspectives on cancer therapeutics. *World J Gastroenterol* 20: 10790–10801
- Tang Z, Li C, Kang B, Gao G, Li C, Zhang Z (2017) GEPIA: a web server for cancer and normal gene expression profiling and interactive analyses. *Nucleic Acids Res* 45: W98–W102
- Thambyrajah R, Mazan M, Patel R, Moignard V, Stefanska M, Marinopoulou E, Li Y, Lancrin C, Clapes T, Möröy T et al (2016) GFI1 proteins orchestrate the emergence of haematopoietic stem cells through recruitment of LSD1. *Nat Cell Biol* 18: 21–32
- Tkach M, Thery C (2016) Communication by extracellular vesicles: where we are and where we need to go. *Cell* 164: 1226–1232
- Ung TH, Madsen HJ, Hellwinkel JE, Lencioni AM, Graner MW (2014) Exosome proteomics reveals transcriptional regulator proteins with potential to mediate downstream pathways. *Cancer Sci* 105: 1384–1392
- Valadi H, Ekstrom K, Bossios A, Sjostrand M, Lee JJ, Lotvall JO (2007) Exosome-mediated transfer of mRNAs and microRNAs is a novel mechanism of genetic exchange between cells. *Nat Cell Biol* 9: 654–659
- Van Cutsem E, Sagaert X, Topal B, Haustermans K, Prenen H (2016) Gastric cancer. *Lancet* 388: 2654–2664
- Van Deun J, Mestdagh P, Agostinis P, Akay Ö, Anand S, Anckaert J, Martinez ZA, Baetens T, Beghein E, Bertier L et al (2017) EV-TRACK: transparent

- reporting and centralizing knowledge in extracellular vesicle research. *Nat Methods* 14: 228–232
- Viklund H, Bernsel A, Skwark M, Elofsson A (2008) SPOCTOPUS: a combined predictor of signal peptides and membrane protein topology. *Bioinformatics* 24: 2928–2929
- Wang J, Hevi S, Kurash JK, Lei H, Gay F, Bajko J, Su H, Sun W, Chang H, Xu G et al (2009) The lysine demethylase LSD1 (KDM1) is required for maintenance of global DNA methylation. *Nat Genet* 41: 125–129
- Wang J, Scully K, Zhu X, Cai L, Zhang J, Prefontaine GG, Kronen A, Ohgi KA, Zhu P, Garcia-Bassets I et al (2007) Opposing LSD1 complexes function in developmental gene activation and repression programmes. *Nature* 446: 882–887
- Wang K, Zhang S, Weber J, Baxter D, Galas DJ (2010) Export of microRNAs and microRNA-protective protein by mammalian cells. *Nucleic Acids Res* 38: 7248–7259
- Yang JK, Song J, Huo HR, Zhao YL, Zhang GY, Zhao ZM, Sun GZ, Jiao BH (2017) DNMT3, p65 and p53 from exosomes represent potential clinical diagnosis markers for glioblastoma multiforme. *Ther Adv Med Oncol* 9: 741–754
- Yokoi A, Villar-Prados A, Oliphant PA, Zhang J, Song X, De Hoff P, Morey R, Liu J, Roszik J, Clise-Dwyer K et al (2019) Mechanisms of nuclear content loading to exosomes. *Sci Adv* 5: eaax8849
- Zhang C, Hoang N, Leng F, Saxena L, Lee L, Alejo S, Qi D, Khal A, Sun H, Lu F et al (2018) LSD1 demethylase and the methyl-binding protein PHF20L1 prevent SET7 methyltransferase-dependent proteolysis of the stem-cell protein SOX2. *J Biol Chem* 293: 3663–3674
- Zhang C, Leng F, Saxena L, Hoang N, Yu J, Alejo S, Lee L, Qi D, Lu F, Sun H et al (2019) Proteolysis of methylated SOX2 protein is regulated by L3MBTL3 and CRL4(DCAF5) ubiquitin ligase. *J Biol Chem* 294: 476–489
- Zhang H, Deng T, Liu R, Bai M, Zhou L, Wang X, Li S, Wang X, Yang H, Li J et al (2017a) Exosome-delivered EGFR regulates liver microenvironment to promote gastric cancer liver metastasis. *Nat Commun* 8: 15016
- Zhang S, Zhao BS, Zhou A, Lin K, Zheng S, Lu Z, Chen Y, Sulman EP, Xie K, Böglér O et al (2017b) m(6)A Demethylase ALKBH5 maintains tumorigenicity of glioblastoma stem-like cells by sustaining FOXM1 expression and cell proliferation program. *Cancer Cell* 31: 591–606.e596
- Zhang X, Lu F, Wang J, Yin F, Xu Z, Qi D, Wu X, Cao Y, Liang W, Liu Y et al (2013) Pluripotent stem cell protein Sox2 confers sensitivity to LSD1 inhibition in cancer cells. *Cell Rep* 5: 445–457
- Zheng YC, Chang J, Zhang T, Suo FZ, Chen XB, Liu Y, Zhao B, Yu B, Liu HM (2017) An overview on screening methods for Lysine Specific Demethylase 1 (LSD1) inhibitors. *Curr Med Chem* 24: 2496–2504
- Zheng Y-C, Duan Y-C, Ma J-L, Xu R-M, Zi X, Lv W-L, Wang M-M, Ye X-W, Zhu S, Mobley D et al (2013) Triazole-dithiocarbamate based selective lysine specific demethylase 1 (LSD1) inactivators inhibit gastric cancer cell growth, invasion, and migration. *J Med Chem* 56: 8543–8560
- Zheng YC, Ma J, Wang Z, Li J, Jiang B, Zhou W, Shi X, Wang X, Zhao W, Liu HM (2015) A systematic review of histone lysine-specific demethylase 1 and its inhibitors. *Med Res Rev* 35: 1032–1071
- Zheng Y-C, Shen D-D, Ren M, Liu X-Q, Wang Z-R, Liu Y, Zhang Q-N, Zhao L-J, Zhao L-J, Ma J-L et al (2016a) Baicalin, a natural LSD1 inhibitor. *Bioorg Chem* 69: 129–131
- Zheng YC, Yu B, Chen ZS, Liu Y, Liu HM (2016b) TCPs: privileged scaffolds for identifying potent LSD1 inhibitors for cancer therapy. *Epigenomics* 8: 651–666
- Zhou A, Lin K, Zhang S, Chen Y, Zhang N, Xue J, Wang Z, Aldape KD, Xie K, Woodgett JR et al (2016) Nuclear GSK3beta promotes tumorigenesis by phosphorylating KDM1A and inducing its deubiquitylation by USP22. *Nat Cell Biol* 18: 954–966